Supporting Information

Adler et al. 10.1073/pnas.1714377115

SI Methods

Considering Different Halfway Points for Signaling, Endocytosis, and Cross-Regulation. We start with the model equations (Eqs. **1**, **2**, **5**, and **6** in the main text) with different halfway points for signaling (k_{ij}) endocytosis (e_{ij}), and cross-regulation (r_{ij}):

$$\dot{X}_1 = X_1\left(\lambda_1\frac{C_{21}}{C_{21}+k_{21}}\left(1-\frac{X_1}{K}\right)-\mu_1\right) \quad [S1]$$

$$\dot{X}_2 = X_2\left(\lambda_2\frac{C_{12}}{C_{12}+k_{12}}-\mu_2\right) \quad [S2]$$

$$\dot{C_{12}} = \beta_{12}X_1\left(1-\frac{1}{2}\theta(1+\theta)+\theta\frac{C_{21}}{C_{21}+r_{21}}\right) + \beta_{22}X_2-\alpha_{12}X_2\frac{C_{12}}{C_{12}+e_{12}}-\gamma C_{12} \quad [S3]$$

$$\dot{C_{21}} = \beta_{21}X_2\left(1-\frac{1}{2}\omega(1+\omega)+\omega\frac{C_{12}}{C_{12}+r_{12}}\right) + \beta_{11}X_1-\alpha_{21}X_1\frac{C_{21}}{C_{21}+e_{21}}-\gamma C_{21}. \quad [S4]$$

Now, the dimensionless equations with the normalized variables, $\tilde{C}_{ij}=C_{ij}/k_{ij}$, depend on four additional parameters: $\tilde{e}_{ij}=e_{ij}/k_{ij}$, $\tilde{r}_{ij}=r_{ij}/k_{ij}$ (for convenience we do not keep the $\sim$ sign):

$$\dot{X}_1 = X_1\left(\lambda_1\frac{C_{21}}{C_{21}+1}(1-X_1)-1\right) \quad [S5]$$

$$\dot{X}_2 = \mu X_2\left(\lambda_2\frac{C_{12}}{C_{12}+1}-1\right) \quad [S6]$$

$$0 = \beta_{12}X_1\left(1-\frac{1}{2}\theta(1+\theta)+\theta\frac{C_{21}}{C_{21}+r_{21}}\right) + \beta_{22}X_2-\alpha_{12}X_2\frac{C_{12}}{C_{12}+e_{12}}-C_{12} \quad [S7]$$

$$0 = X_2\left(1-\frac{1}{2}\omega(1+\omega)+\omega\frac{C_{12}}{C_{12}+r_{12}}\right) + \beta_{11}X_1-\alpha_{21}X_1\frac{C_{21}}{C_{21}+e_{21}}-C_{21}. \quad [S8]$$

Solving for the nullclines yields

$$X_2 = \frac{(\lambda_2-1)e_{12}+1}{\alpha_{12}-((\lambda_2-1)e_{12}+1)\beta_{22}} \times\left(\frac{1}{1-\lambda_2}+X_1\left(1-\frac{\theta}{2}(1+\theta)+\frac{\theta}{1-r_{21}+r_{21}\lambda_1(1-X_1)}\right)\right) \quad [S9]$$

$$X_2 = \frac{2(1+\mathrm{r}_{12}(\lambda_2-1))\left(X_1\left(\beta_{11}-\frac{\alpha_{21}}{1-e_{21}+e_{21}\lambda_1(1-X_1)}\right)+\frac{1}{1-\lambda_1(1-X_1)}\right)}{(-2\omega+(1+\mathrm{r}_{12}(\lambda_2-1))(-2+\omega+\omega^2))}. \quad [S10]$$

The nullclines described in the main text (Eqs. **24** and **25** in *Methods*) are with $e_{ij}, r_{ij}=1$. Having different values for e_{ij}, r_{ij} may change the position of the fixed points but has small effect on the shape of the nullclines and therefore does not affect the stability.

Proof that Down-Regulation on C_{12} Is Necessary and Sufficient for the Existence of Parameters Under Which the Circuit Has an ON State. First, we show that the zero fixed point, $X_1, X_2=0$, is stable for all circuits, meaning that a small deviation away from the OFF state eventually flows back to it. The eigenvalues (ev_i) of the system (Eqs. **16**–**19** in *Methods*) in the OFF state where the cells and GFs are zero are negative for all circuits and all values of parameters: $ev_1=ev_2=ev_3=-1, ev_4=-\mu$. Therefore, the OFF state is always stable and has a certain basin of attraction.

Let us assume that there is no down-regulation on C_{12}. Therefore, X_2 does not endocytose C_{12}, $a_{12}=0$, and the other GF, C_{21}, does not cross-inhibit C_{12} gene expression, $\theta\neq -1$.

We now show that in the absence of down-regulation on C_{12} there is no finite ON-state solution. The cells will either flow to the OFF state or grow until X_1 reaches their carrying capacity and X_2 reaches carrying capacity that is not introduced in the model.

We will prove this by analyzing the stability of each fixed point using the following approach: We compute the direction of the flow of the cell numbers $(\dot{X}_1, \dot{X}_2)$ on every region on the phase portrait, where each region differs in the sign of the derivatives of the cell numbers. Using these flows, we can determine whether the fixed points are stable or not (see ref. 1, section 6).

We will separate the proof for the case of $\beta_{22}=0$ and for the case $\beta_{22}\neq 0$.

If $\beta_{22}=0$, without endocytosis the first nullcline (Eq. **24** in *Methods*) is not defined since it is divided by zero. Therefore, we need to go back to the original equation for the first nullcline (Eq. **20** in *Methods*) and substitute there $\beta_{22}, \alpha_{12}=0$:

$$0 = X_1\left(1-\frac{1}{2}\theta(1+\theta)+\frac{\theta}{\lambda_1(1-X_1)}\right)-\frac{1}{\lambda_2-1}. \quad [S11]$$

Note that Eq. **S11** does not depend on X_2, and therefore this nullcline is solved independently of X_2. For $\theta=0, 1$ Eq. **S11** yields a single solution for X_1:

$$X_1 = \frac{\theta(\lambda_1-1)+1}{\lambda_1\theta+\lambda_2-1}. \quad [S12]$$

Since there is only a single solution for X_1, this nullcline can intersect the second nullcline (Eq. **25** in *Methods*) at a single point. This fixed point is unstable, because the zero fixed point is always stable as we showed previously (Fig. S3*A*).

If $\beta_{22}\neq 0$, without endocytosis we can use Eq. **24** (in *Methods*) for the first nullcline, which becomes a decreasing function in X_1:

$$X_2 = -\frac{1}{\beta_{22}}\left(\frac{1}{1-\lambda_2}+X_1\right), \text{ for } \theta=0 \quad [S13]$$

$$X_2 = -\frac{1}{\beta_{22}}\left(\frac{1}{1-\lambda_2}+\frac{1}{\lambda_1}\frac{X_1}{1-X_1}\right), \text{ for } \theta=1. \quad [S14]$$

The second nullcline (Eq. **25** in *Methods*) is a curve that diverges to infinity as $X_1\to(1-1/\lambda_1)$. This curve behaves differently for small X_1 depending on three regimes of the autocrine secretion rate, β_{11}.

If $\beta_{11}<A$, $A\equiv\lambda_1/(\lambda_1-1)^2+\alpha_{21}/\lambda_1$, then the second nullcline is a positive monotonic increasing function in X_1. Recall that the

first nullcline (Eqs. **S13** and **S14**) is a decreasing function of X_1. Therefore, there is only one possible intersection point between the two nullclines, which is unstable due to the stability of the zero fixed point (Fig. S3*B*).

There exists a value, B, such that $A<B$. If $A<\beta_{11}<B$, the second nullcline is a positive hyperbolic function which decreases for $X_1<<1$ and increases for larger values of X_1, diverging as $X_1\to(1-1/\lambda_1)$. In this case, the two nullclines may intersect twice, but we show graphically that the two fixed points are unstable (Fig. S3*C*).

If $\beta_{11}>B$, then the second nullcline has the same shape as the previous case only now it becomes negative for a certain intermediate range of X_1 and therefore will intersect the nullcline, $X_2=0$, twice. Graphically, one can see that the intermediate intersection with $X_2=0$ is unstable and the higher intersection (larger X_1) is stable. This leads to the fact that the intersection points between the two curved nullclines are unstable as well (Fig. S3*D*).

To summarize, we showed that in the lack of down-regulation on C_{12} there is no stable ON state.

We now show that introducing either endocytosis of C_{12}, namely $\alpha_{12}>0$, or down-regulation by C_{21} (in the absence of autocrine of C_{12}), namely $\theta=-1$, is sufficient for a certain range of parameters in which there is a stable ON state.

If $\alpha_{12}>0$, the nullcines (Eqs. **24** and **25** in *Methods*) become

$$X_2=\frac{\lambda_2}{\alpha_{12}-\lambda_2\beta_{22}}\left(\frac{1}{1-\lambda_2}+X_1\left(1-\frac{\theta}{2}(1+\theta)+\frac{\theta}{\lambda_1(1-X_1)}\right)\right) \quad \textbf{[S15]}$$

$$X_2=\frac{2\lambda_2\left(X_1\left(\beta_{11}-\frac{\alpha_{21}}{\lambda_1(1-X_1)}\right)+\frac{1}{1-\lambda_1(1-X_1)}\right)}{(-2\omega+\lambda_2(-2+\omega+\omega^2))}. \quad \textbf{[S16]}$$

The first nullcline (Eq. **S15**) is a nonmonotonic function of X_1 that first rises and then declines with X_1 for $\theta=-1$ (Fig. S3*E*), a linear increasing line for $\theta=0$ (Fig. S3*F*), and an increasing curve for $\theta=1$ (Fig. S3*G*). For all values of θ,ω there is a range of parameters in which the two nullclines intersect twice, and therefore there is a stable ON state (Fig. S3 *E*–*G*). This can be seen by considering the points where the nullclines cross the X_2 axis, meaning substituting $X_1=0$ in Eqs. **S15** and **S16**. There is a range of parameters (e.g., large α_{12}) in which the point on the X_2 axis of the second nullcline (Eq. **S16**) is larger than the point on the X_2 axis of the first nullcline (Eq. **S15**). There is also a range of parameters (large β_{11}) in which the second nullcline (Eq. **S16**) becomes negative for an intermediate range of X_1, and then it rises and diverges at $X_1\to(1-1/\lambda_1)$. Therefore, the nullclines must intersect twice for this range of parameters.

If $\alpha_{12}=0,\theta=-1$, the first nullcline (Eq. **S15**) becomes (for $\beta_{22}\neq 0$)

$$X_2=\frac{1}{\beta_{22}}\left(\frac{1}{\lambda_2-1}-X_1\left(1-\frac{1}{\lambda_1(1-X_1)}\right)\right). \quad \textbf{[S17]}$$

This curve (Eq. **S17**) is a nonmonotonic function of X_1 that first declines and then increases with X_1. Therefore, for some range of parameters it will cross the other nullcline (Eq. **S16**), which is an increasing function of X_1, three times. These intersection points are unstable (Fig. S3*H*). Therefore, in the case of no endocytosis, having autocrine on C_{12} breaks the stability.

If there is no autocrine secretion of C_{12}, namely $\beta_{22}=0$, the equation for the first nullcline (Eq. **S15**) becomes

$$0=X_1\left(1-\frac{1}{\lambda_1(1-X_1)}\right)-\frac{1}{\lambda_2-1}. \quad \textbf{[S18]}$$

This equation is independent of X_2 and has two solutions for X_1:

$$X_1=\frac{\lambda_1+(\lambda_1-1)(\lambda_2-1)\mp\sqrt{(\lambda_1+(\lambda_1-1)(\lambda_2-1))^2+4\lambda_1(\lambda_1-\lambda_1\lambda_2)}}{2\lambda_1(\lambda_2-1)}. \quad \textbf{[S19]}$$

The two solutions for X_1 (Eq. **S19**) are both positive for $2\sqrt{\lambda_1^3/(-1+\lambda_1)^4(-1+\lambda_2)^2+\lambda_1+\lambda_1^2/(-1+\lambda_1)^2(-1+\lambda_2)}\leq 1$. Therefore, for a certain range of parameters we have two intersection points between the two nullclines—the first is unstable and the second is the stable ON state (Fig. S3*I*).

To summarize, down-regulation on C_{12} by C_{21} (in the absence of autocrine on C_{12}) or endocytosis of C_{12} is sufficient for a stable ON state for a certain range of parameters.

Two-Cell Circuits Where Both Cells Are Far from Carrying Capacity Cannot Reach Stable ON State. We model two-cell circuits similar to the model presented in the main text (Eqs. **16**–**19** in *Methods*) only without the carrying capacity term for X_1:

$$\dot{X}_1=X_1(\lambda_1 h(C_{21})-1) \quad \textbf{[S20]}$$

$$\dot{X}_2=X_2\mu(\lambda_2 h(C_{12})-1) \quad \textbf{[S21]}$$

$$0=\beta_{12}X_1\left(1-\frac{1}{2}\theta(1+\theta)+\theta h(C_{21})\right)+\beta_{22}X_2-\alpha_{12}X_2h(C_{12})-C_{12} \quad \textbf{[S22]}$$

$$0=X_2\left(1-\frac{1}{2}\omega(1+\omega)+\omega h(C_{12})\right)+\beta_{11}X_1-\alpha_{21}X_1h(C_{21})-C_{21}. \quad \textbf{[S23]}$$

The nullclines for these circuits are now

$$X_2=\frac{\lambda_2}{\alpha_{12}-\lambda_2\beta_{22}}\left(\frac{1}{1-\lambda_2}+X_1\left(1-\frac{\theta}{2}(1+\theta)+\frac{\theta}{\lambda_1}\right)\beta_{12}\right) \quad \textbf{[S24]}$$

$$X_2=\frac{2\lambda_2(X_1(\alpha_{21}-\lambda_1\beta_{11})(1-\lambda_1)-\lambda_1)}{\lambda_1(-2\omega+\lambda_2(-2+\omega+\omega^2))(\lambda_1-1)}. \quad \textbf{[S25]}$$

These nullclines are simply the nullclines of the original model (Eqs. **24** and **25** in *Methods*), when taking the limit of X_1 cells that are far below their carrying capacity, $X_1<<1$.

Both nullclines (Eqs. **24** and **25**) are linear in X_1 and therefore can intersect only once (except for the points where $X_1=0$ or $X_2=0$). There are five different cases for the way these two lines cross: one of them decreases and the other one increases, or vice versa, both are increasing, and both are decreasing where one line intersect the x_2 axis higher than the other, and vice versa. In all five cases the intersection point is not stable, as can be seen in the phase portraits (Fig. S3 *J*–*N*).

Explicit Modeling of Receptor Internalization. Receptors, such as the CSF1 receptor and the PDGF receptor, are usually internalized and degraded together with their ligand. To model this, we introduce an equation for the receptors R_i, made by X_i cells and where removal is due to internalization due to binding of the GF, C_{ji}, and to receptor degradation-dilution at rate α_{Ri} [degradation rate is typically on order of 1/h (2–4), exceeding the effects of dilution by cell growth]:

$$\frac{dR_i}{dt}=\beta_{Ri}-\alpha_{ji}h(C_{ji})R_i-\alpha_{Ri}R_i. \quad \textbf{[S26]}$$

The equation for the ligand C_{ji} is a balance of production at rate β_{ji} from cells X_j and the same internalization rate (due to the stoichiometry in which ligand and receptor are internalized together):

$$\frac{dC_{ji}}{dt}=\beta_{ji}X_j f\left(\frac{R_i}{R_{i,T}},h(C_{ij}),\theta\right)-\alpha_{ji}h(C_{ji})R_iX_i-\gamma C_{ji}, \qquad \text{[S27]}$$

where $f(R_i/R_{i,T},h(C_{ij}),\theta)=\{R_i/R_{i,T}(1-h(C_{ij})),1,R_i/R_{i,T}h(C_{ij})\}$ for $\theta=\{-1,0,1\}$ respectively describes the cross-regulation due to the other GF C_{ij} signaling which depends on the fraction of free receptors on the cell surface, $R_i/R_{i,T}$, where $R_{i,T}\equiv\beta_{Ri}/\alpha_{Ri}$ is the amount of receptors per cell when there is no endocytosis, $\alpha_{ji}=0$.

The equation for the cell X_i is a balance of proliferation and removal as before where the proliferation term is multiplied by the signaling factor, $R_i/R_{i,T}h(C_{ji})$:

$$\frac{dX_i}{dt}=X_i\left(\lambda_i\frac{R_i}{R_{i,T}}h(C_{ji})\left(1-\frac{X_i}{K_i}\right)-\mu_i\right). \qquad \text{[S28]}$$

Using the fact that receptor and GF removal rates are faster than cell removal rates, we can consider the steady state of the receptor, $R_{i,st}$, in the signaling factor and in the internalization term: $R_{i,st}h(C_{ji})=\beta_{Ri}/(\alpha_{ji}(C_{ji}/k_{ji}+C_{ji})+\alpha_{Ri})C_{ji}/(k_{ji}+C_{ji})=\beta_{Ri}/(\alpha_{Ri}+\alpha_{ji})C_{ji}/(\alpha_{Ri}/(\alpha_{Ri}+\alpha_{ji})k_{ji}+C_{ji})$.

Thus, we get a Michaelis–Menten function of the GF with a new halfway point, $\tilde{k}_{ji}=\alpha_{Ri}/(\alpha_{Ri}+\alpha_{ji})k_{ji}$, and a prefactor, $\beta_{Ri}/(\alpha_{Ri}+\alpha_{ji})$, that can be collapsed into the model rate parameters.

To simulate this, we consider the dimensionless equations where the dimensionless variables for the GFs and cells are as described in *Methods* and the receptors $\tilde{R}_i=R_i/(\beta_{Ri}/\alpha_{Ri})$ (for convenience we do not keep the $\sim$ sign):

$$\frac{\mu_1}{\alpha_{R1}}\frac{dR_1}{dt}=1-\frac{\alpha_{21}}{\alpha_{R1}}h(C_{21})R_1-R_1 \qquad \text{[S29]}$$

$$\frac{\mu_1}{\alpha_{R2}}\frac{dR_2}{dt}=1-\frac{\alpha_{12}}{\alpha_{R2}}h(C_{12})R_2-R_2 \qquad \text{[S30]}$$

$$\frac{\mu_1}{\gamma}\frac{dC_{12}}{dt}=\tilde{\beta}_{12}X_1f(R_1,h(C_{21}),\theta)-\tilde{\alpha}_{12}h(C_{12})R_2X_2-C_{12} \qquad \text{[S31]}$$

$$\frac{\mu_1}{\gamma}\frac{dC_{21}}{dt}=X_2f(R_1,h(C_{12}),\omega)-\tilde{\alpha}_{21}h(C_{21})R_1X_1-C_{21} \qquad \text{[S32]}$$

$$\frac{dX_1}{dt}=X_1\left(\tilde{\lambda}_1R_1h(C_{21})(1-X_1)-\tilde{\mu}_1\right) \qquad \text{[S33]}$$

$$\frac{dX_2}{dt}=\tilde{\mu}X_2\left(\tilde{\lambda}_2R_2h(C_{12})-\tilde{\mu}_2\right). \qquad \text{[S34]}$$

We use the fact that the timescale of cells in much slower than the timescale of receptors and GFs to set Eqs. **S29**–**S32** to zero. Therefore, there are two more dimensionless parameters when we consider receptor internalization: $\alpha_1=\alpha_{21}/\alpha_{R1}$ and $\alpha_2=\alpha_{12}/\alpha_{R2}$. In Fig. S5*B* we plot the phase portrait of this system (Eqs. **S29**–**S34**) for the same dimensionless parameters as in Fig. 1*E* only with slightly adjusted proliferation to removal rate ratios, $\tilde{\lambda}_i$, which are still within the biological plausible range, and for equal GF internalization and receptor removal rates ($\alpha_i=1$), which results in very similar phase portrait as in Fig. 1*E* (Fig. S5*B*).

1. Strogatz SH (2014) *Nonlinear Dynamics and Chaos: With Applications to Physics, Biology, Chemistry, and Engineering* (Westview, Boulder, CO).
2. Lee PSW, et al. (1999) The Cbl protooncoprotein stimulates CSF-1 receptor multiubiquitination and endocytosis, and attenuates macrophage proliferation. *EMBO J* 18: 3616–3628.
3. Yu W, et al. (2012) Macrophage proliferation is regulated through CSF-1 receptor tyrosines 544, 559, and 807. *J Biol Chem* 287:13694–13704.
4. Krupp MN, Connolly DT, Lane MD (1982) Synthesis, turnover, and down-regulation of epidermal growth factor receptors in human A431 epidermoid carcinoma cells and skin fibroblasts. *J Biol Chem* 257:11489–11496.

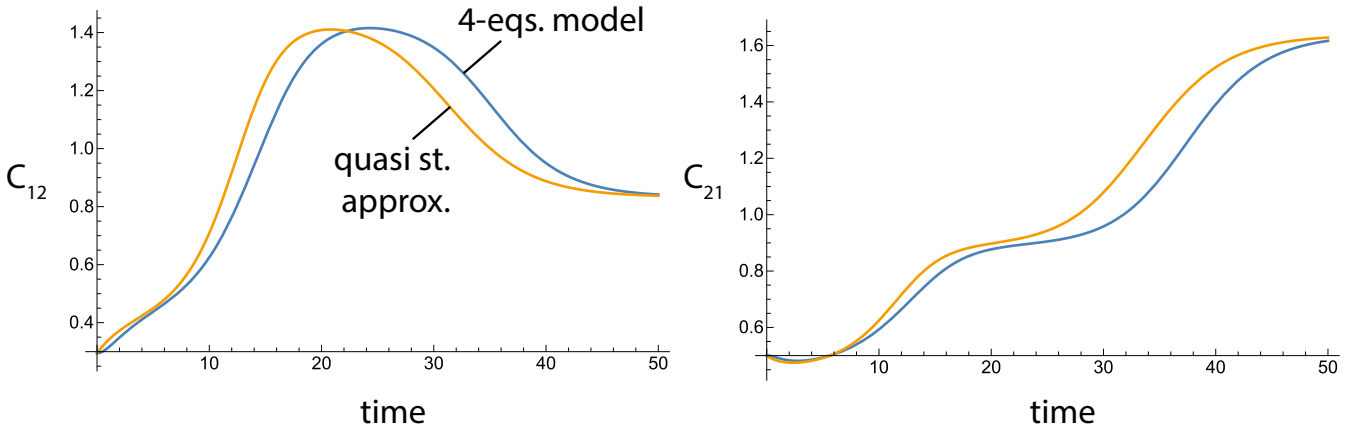

Fig. S1. Dynamics of the GF concentration calculated by solving numerically the four-equation model (Eqs. **1**–**4** in *Results* section, in blue) and by solving the equations for the cells (Eqs. **1** and **2** in *Results*) while considering a quasi-steady state for the GFs (setting Eqs. **3** and **4** in *Results* to zero, in orange).

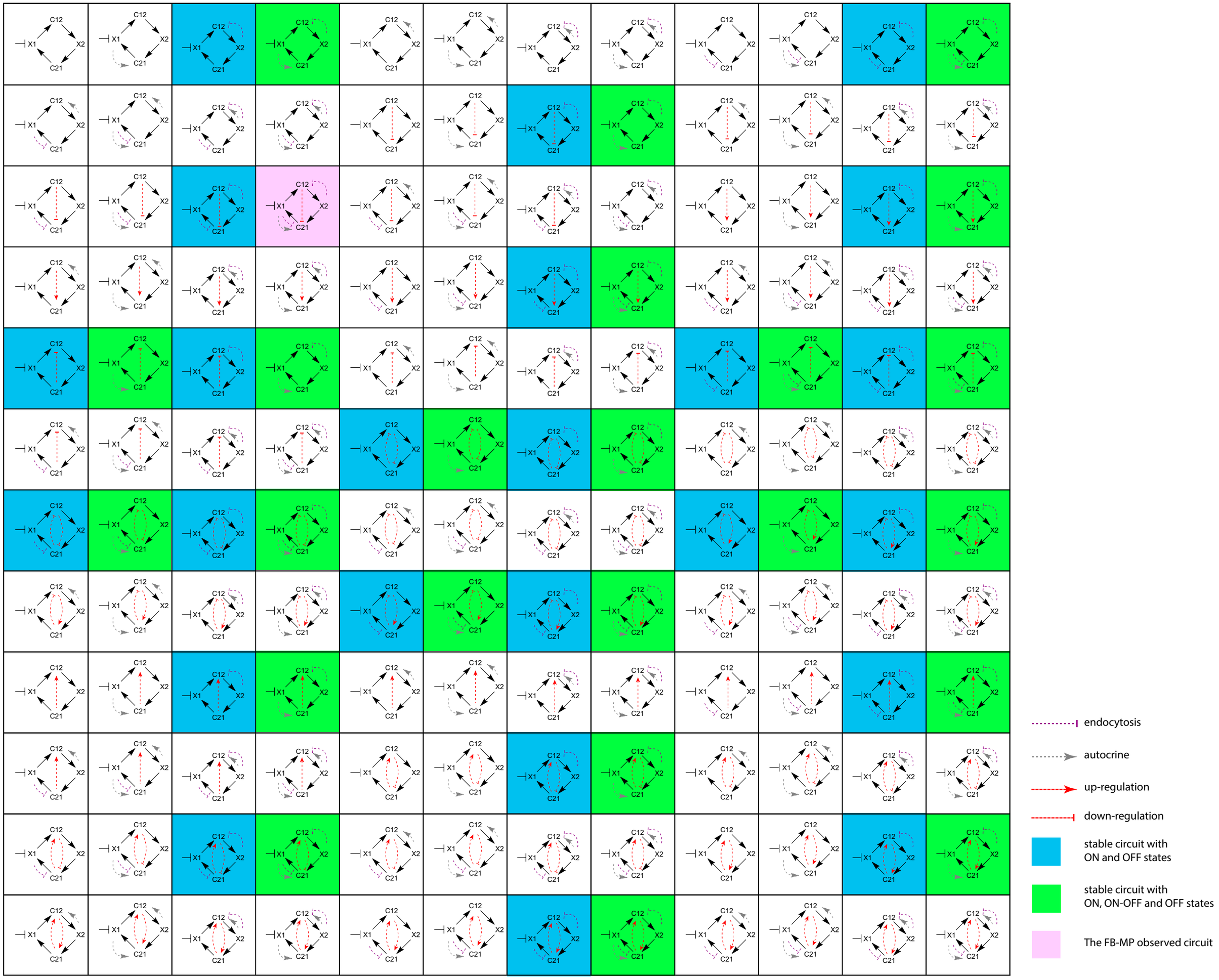

Fig. S2. All 144 possible two-cell circuits in the two-cell circuit screen with the 48 stable circuits marked. The 24 circuits that show also the ON–OFF state are marked in green, and the observed FB–MP circuit marked in light purple.

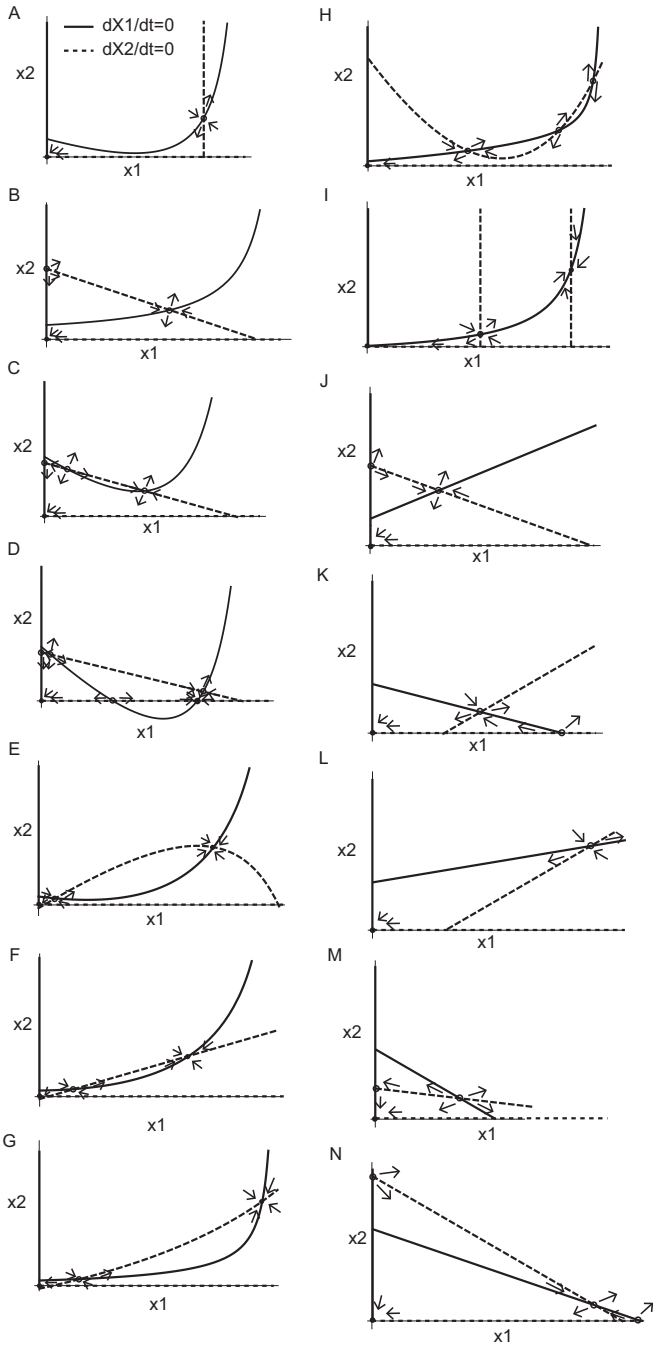

Fig. S3. (*A*–*N*) Phase portraits showing the nullclines of the two-cell circuits for different interactions and conditions on the parameters.

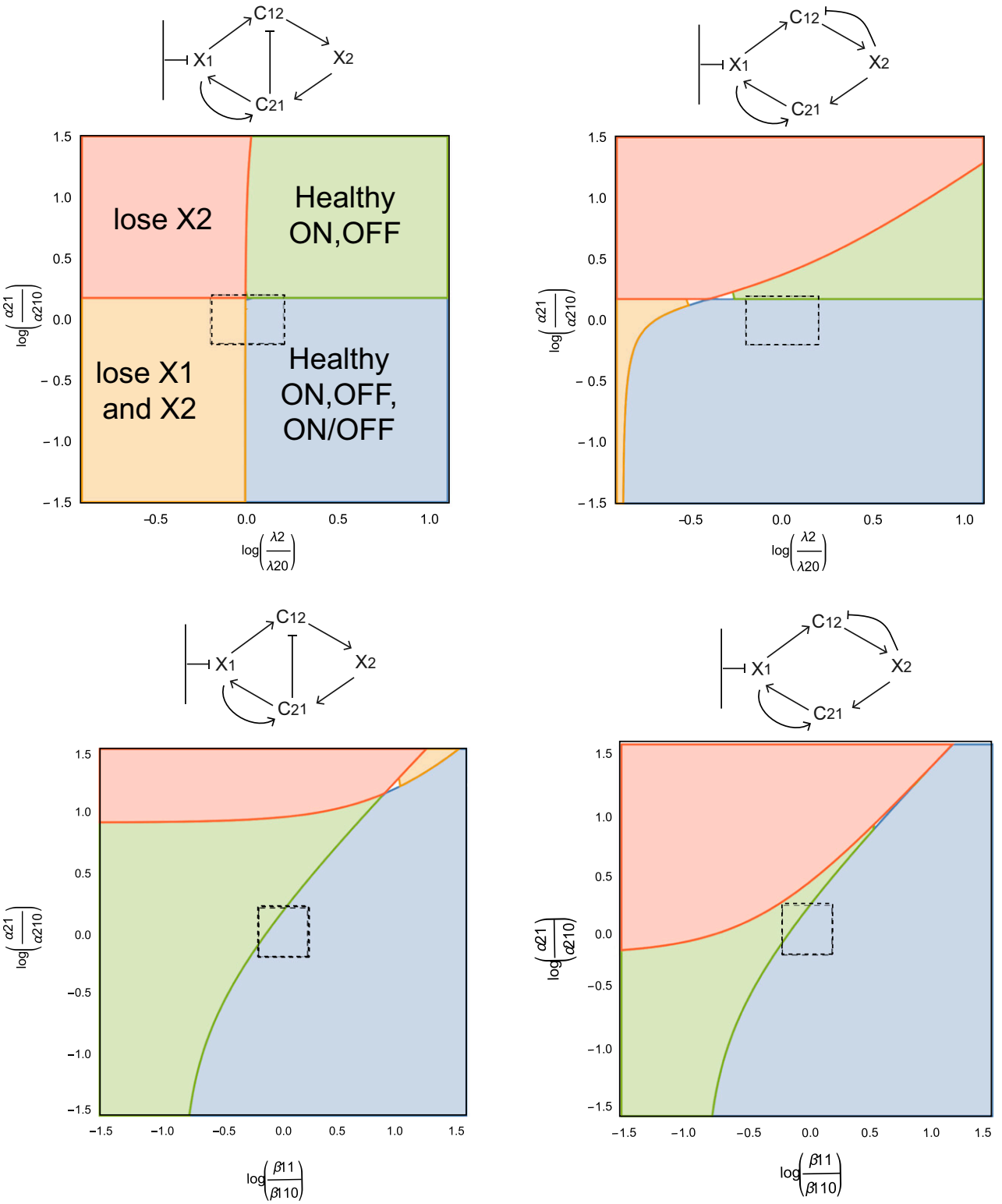

Fig. S4. Two more combinations of parameters from the model showing how many fixed points the two-cell circuits have in these parameter ranges.

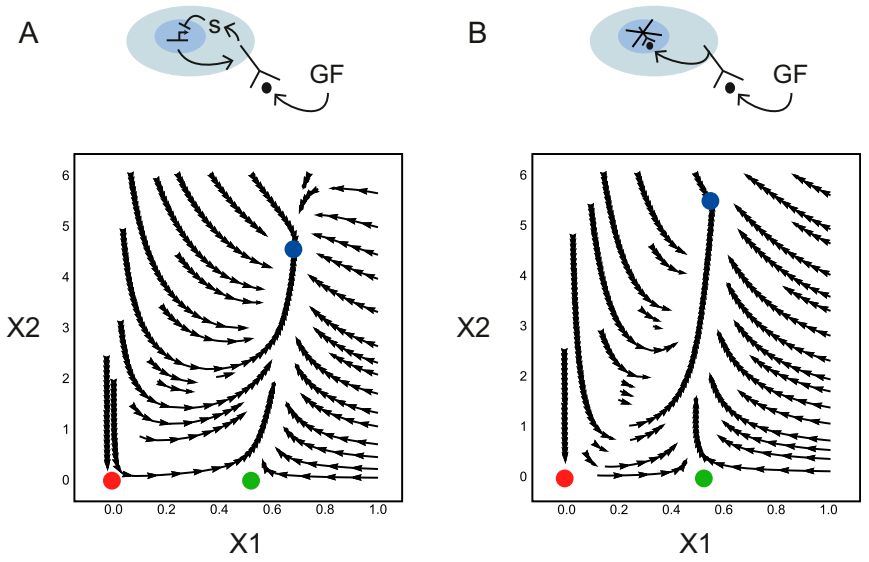

Fig. S5. (*A*) Simulations of the observed FB–MP circuit with a negative feedback on the GF receptor levels with the same dimensionless parameters as in Fig. 1*E*. (*B*) Phase portrait of the observed FB–MP circuit with receptor internalization through endocytosis with the same dimensionless parameters as in Fig. 1*E* only with $\tilde{\lambda}_1 = 5, \tilde{\lambda}_2 = 4$ and $\alpha_1 = \alpha_2 = 1$.

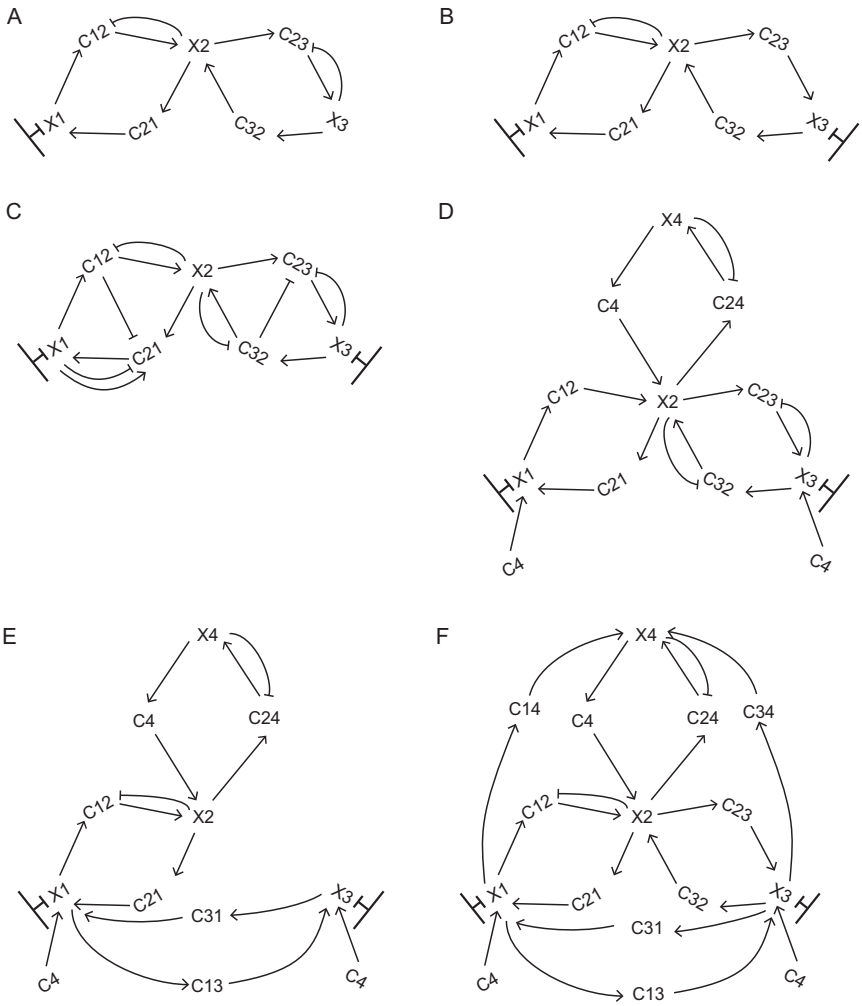

Fig. S6. (*A–C*) Three additional three-cell circuits and (*D–F*) three additional four-cell circuits that implement our hypothesized generalized condition for stability show a stable ON state of all cell types.